Toward the Mechanistic Understanding of the Additives' Role on Ammonium Nitrate Decomposition: Calcium Carbonate and Calcium Sulfate as Case Studies

Eleonora Menicacci, Patricia Rotureau, Guillaume Fayet, Carlo Adamo

ACS OMEGA

http://pubs.acs.org/journal/acsodf

Article

Toward the Mechanistic Understanding of the Additives' Role on Ammonium Nitrate Decomposition: Calcium Carbonate and Calcium Sulfate as Case Studies

Eleonora Menicacci, Patricia Rotureau,* Guillaume Fayet, and Carlo Adamo*

Cite This: *ACS Omega* 2020, 5, 5034−5040

Read Online

ACCESS | Metrics & More | Article Recommendations | Supporting Information

ABSTRACT: The reaction mechanism involved in the decomposition of ammonium nitrate (AN) in the presence of $CaCO_3$ and $CaSO_4$, commonly used for stabilization and the reduction of explosivity properties of AN, was theoretically investigated using a computational approach based on density functional theory. The presented computational results suggest that both carbonate and sulfate anions can intercept an acid proton from nitric acid issued from the first step of decomposition of AN, thus inhibiting its runaway decomposition and the generation of reactive species (radicals). The reaction then leads to the production of stable products, as experimentally observed. Our modeling outcomes allow for tracing a relationship between the capability of proton acceptance of both carbonate and sulfate anions and the macroscopic behavior of these two additives as inhibitor or inert in the AN mixture.

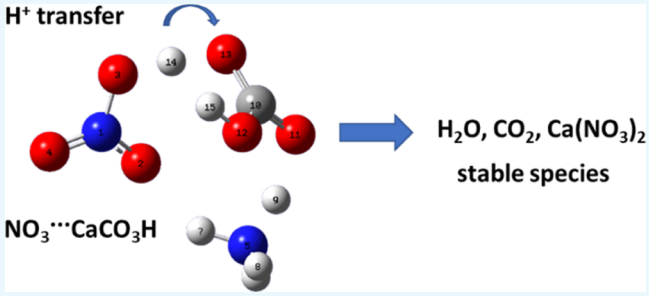

1. INTRODUCTION

Ammonium nitrate (AN) is widely used in the industry. For instance, it is a source of nitrogen in fertilizer formulations, and it is also employed as a combustible in explosives because of its remarkable oxidant properties. The safety knowledge about AN is essentially based on the feedback coming from past accidents and experimental studies, the latter being mainly calorimetric and kinetic studies.[1−5] AN is described as presenting good chemical stability when it is correctly manufactured, uncontaminated, and stored under adequate conditions. Nevertheless, AN can undergo fast decomposition[6−9] in certain situations (e.g., under confinement or in the presence of contaminants), leading to major accidents during production and storage.[10,11]

Because AN-based fertilizers always contain additives for a variety of reasons (e.g., efficient granulation or prilling, anticaking effect, slow release of nutriment at end-use, etc...), it is important to fully understand their influence on the thermal stability of the resulting mixtures. Starting from calorimetric tests,[12−16] previous works[17−19] identified different behaviors of additives on the thermal stability of AN formulations, leading to three different classes: promoters, inert substances, and inhibitors. A promoter (or incompatible) substance causes destabilization of AN, and it is experimentally identified by a decrease of the decomposition temperature of the mixture with respect to that of pure AN, often associated with a higher energy release during the decomposition.[17−19] Examples of promoters are fuels, halide salts, nitrates and sulfates of chromium, iron, copper, and aluminum, and several organic compounds.[20,21] An inert additive (apparently) does not affect the thermal stability of AN because no significant temperature shift of the exothermal decomposition is observed [e.g., for $NaNO_3$, KNO_3 and $Ca(NO_3)_2$].[20,21] It generally acts through a physical dilution effect, reducing the heat released during the (possible) explosive decomposition of the formulation.[20] An inhibitor has a stabilizing effect on AN, leading to a higher decomposition temperature of the mixture and a lower heat release during the reaction than those observed for neat AN.[17−21] Most of the salts of oxyanions ($A_xO_y^{z-}$) such as sulfates, carbonates, or phosphates of sodium, potassium, ammonium, and calcium evidenced such behavior when investigated by differential scanning calorimetry (DSC).[20]

For instance, it is well known that calcium carbonate shows remarkable inhibiting properties when mixed in limited quantities with AN, as recently reported by Babrauskas in the case of AN-based fertilizer formulations.[11] Indeed, he showed that the explosive power developed by a mixture of AN/calcium carbonate (90/10) is only 10% of the reference (picric acid, a primary explosive), whereas neat AN would achieve 80%. Accordingly, this inhibitor property is extensively

Received: November 20, 2019
Accepted: February 25, 2020
Published: March 9, 2020

https://dx.doi.org/10.1021/acsomega.9b03964
ACS Omega 2020, 5, 5034−5040

used by manufacturers to market the so-called CAN fertilizer formulation (CAN stands for calcium ammonium nitrate), which is considered significantly safer than conventional AN formulations containing up to 33−34% nitrogen from AN (although not exempt of any explosion hazard).

Even if calorimetric tests provide valuable information on the global effect of additives on the thermal stability of AN, they do not allow a clear identification of the detailed reaction mechanism involved in the AN decomposition. To (partially) fill this gap, a molecular modeling approach was proposed to clarify the detailed reaction mechanism of incompatible substances with AN.[22−24] In particular, this approach was successfully used to investigate the incompatibility of sodium salt of dichloroisocyanuric acid.[23] Whereas the proposed mechanism for the chemical incompatibility of AN has been validated for other chemicals,[24] still no evidence has been given on how other compatible (i.e., inhibitor and inert) compounds act on the AN decomposition.

Among the substance classified as inhibitors, calcium carbonate ($CaCO_3$) is widely used because it ensures excellent stabilization capabilities[20] and it can be obtained at low cost from dolomite and limestone.[25] Several experimental studies have been conducted, leading to the proposition of the following reaction for the decomposition of AN in the presence of $CaCO_3$[25−30]

$$2NH_4NO_3 + CaCO_3 \rightarrow Ca(NO_3)_2 + 2NH_3 + H_2O + CO_2 \quad (1)$$

Experimental calorimetric tests also demonstrated the inhibitor behavior of this salt. Typical parameters to rationalize the behavior of the mixture with respect to pure compound are the onset temperature (T_{onset}), that is, the temperature at which the calorimetric reaction starts, and the maximum temperature (T_{max}), corresponding to the maximum of the peak of the calorimetric plot. For the decomposition of pure AN, this last temperature is 263.0 °C with differential thermal analysis experiments, whereas it ranges between 270.7 and 308.8 °C when it is mixed with 5% wt of different types of dolomite and limestone.[29] DSC experiments indicate that T_{max} of decomposition of pure AN is 326 °C, a value that increases to 360.0 °C, when mixed with 5% wt of pure $CaCO_3$, and to 389.0 °C with 20%.[29] The decomposition of pure AN generates a heat of 1255 J/g, but when it is mixed with 33% wt of $CaCO_3$, the heat generated decreases to 397 J/g. The ensemble of these data clearly shows the inhibiting behavior of calcium carbonate and its role as a robust stabilizer of AN formulations.

Contrary to $CaCO_3$, only limited literature exists on $CaSO_4$, and it suggests a lower stabilizing effect on the thermal stability of AN.[20,21] Indeed, according to DSC tests,[20] T_{max} increases to 333.0 °C when AN is mixed with 5% wt of pure $CaSO_4$, and with 20% wt of $CaSO_4$, T_{max} is 334 °C. Moreover, the heat generated by a mixture of AN with 33% weight of $CaSO_4$ is 669 J/g, about one-half of AN decomposition heat.

Considering all these experimental data, we have investigated, using modern modeling techniques, the decomposition of AN in the presence of $CaCO_3$ and $CaSO_4$ in order to shed light on the underpinning molecular reaction mechanisms. In particular, our work is aimed at identifying the role played by $CaCO_3$ and $CaSO_4$ on the decomposition pathway of AN in reducing, or even eliminating, the generation of highly reactive species (such as radicals or energetic molecules). Furthermore, an effort was made to define a relationship between the key reaction steps of the identified reactions and the behavior, as inert or inhibitor, of $CaCO_3$ and $CaSO_4$ when added to the AN mixture.

2. RESULTS AND DISCUSSION

Our previous study[22] revealed that the rate-determining step of AN decomposition requires a significant amount of energy, and it leads to the production of a number of reactive species. After the first step, where AN can easily dissociate (ΔG = 5.4 kcal/mol) into NH_3 and HNO_3 (eq 2), nitrogen dioxide ($NO_2^{\bullet}$) and hydroxyl ($OH^{\bullet}$) radicals are formed through homolytic rupture of the NO bond (eq 3).

$$NH_4NO_3 \rightarrow NH_3 + HNO_3 \quad (2)$$

$$HNO_3 \rightarrow OH^{\bullet} + NO_2^{\bullet} \quad (3)$$

This last reaction is the rate-limiting step of AN decomposition, and it requires a high amount of energy (ΔG = 40.2 kcal/mol),[22] which explains the stability of AN under normal conditions of storage. The whole decomposition process is, however, strongly exothermic with the release of a high amount of energy (ΔG = −165 kcal/mol). The final products, in agreement with experimental observations, are N_2, H_2O, O_2, OH, HNO, and NO_3.

In the following, we assume that reaction 2 has already taken place because it requires a small amount of energy and, therefore, attention will be given to the possible reactions of $CaCO_3$ and $CaSO_4$ with HNO_3 or NH_3. We will then compare these reactions with the decomposition of pure AN in order to identify the energetically most favorable decomposition pathway and the related products.

It should be considered that all calculations presented in the following were carried out in the gas phase, whereas the experimental conditions could be affected by some factors such as atmosphere components (including humidity), impurities, or aggregation state. These effects require dedicated modeling approaches: for instance, amorphous inorganic substances can be modelled using periodic boundary conditions for ideal crystals (see for instance refs 31−34) and the effect of the moisture can be simulated by the introduction of a finite number of water molecules in the reaction mechanisms (as in ref 23). Exploring all these effects is, therefore, not only complex from a computational point of view (and out of the scope of the present paper) but also requires a preliminary knowledge of the basic (unperturbed) reaction mechanisms, whose identification is the aim of the present paper. This is even more necessary when the reactions take place in "real life" environments and all experimental conditions are difficult to assess. Therefore, despite the model limitations, the theoretical characterization of the gas-phase molecules and the reaction provides valuable hints on the elementary chemical processes involving energetic materials,[22,23,35−37] especially when it can be related to experimental evidences, such as the identified stable products.

2.1. Reaction Mechanism between AN and $CaCO_3$.

The reaction between AN and $CaCO_3$ was investigated by considering that $CaCO_3$ can separately react with nitric acid, here after referred to as path A, and ammonia, path B. The whole reaction mechanism is reported in Scheme 1, and the corresponding energy profile is in Figure 1. The computed energies are also reported in Table 1.

https://dx.doi.org/10.1021/acsomega.9b03964
ACS Omega 2020, 5, 5034−5040

Scheme 1. Pathway of Reactions between AN and $CaCO_3$

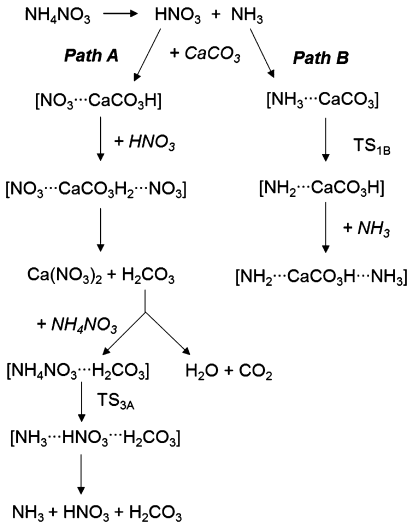

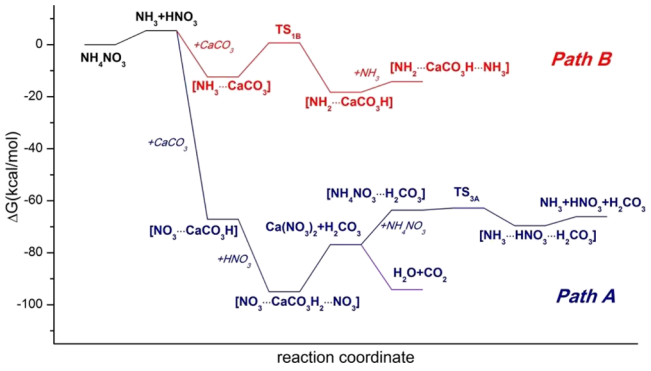

Figure 1. Gibbs free-energy profile for the reaction between AN and $CaCO_3$.

Table 1. Relative Energies (kcal/mol) for the Decomposition Reaction of NH_4NO_3 in the Presence of $CaCO_3$

	ΔE	ΔH	ΔG
NH_4NO_3	0.0	0.0	0.0
$NH_3 + HNO_3$	13.5	14.0	5.4
Path A			
$[NO_3\cdots CaCO_3H]$	−69.4	−68.5	−67.1
$[NO_3\cdots CaCO_3H_2\cdots NO_3]$	−108.8	−108.0	−95.0
$Ca(NO_3)_2 + H_2CO_3$	−80.5	−79.9	−76.9
$[NH_4NO_3\cdots H_2CO_3]$	−71.8	−71.3	−63.6
TS_{3A}	−70.7	−70.4	−62.8
$[NH_3\cdots HNO_3\cdots H_2CO_3]$	−76.1	−75.0	−69.6
$NH_3 + HNO_3 + H_2CO_3$	−53.5	−52.0	−66.1
$H_2O + CO_2$	−89.7	−87.4	−94.2
Path B			
$[NH_3\cdots CaCO_3]$	−12.8	−12.8	−12.4
TS_{1B}	−0.9	−1.5	0.7
$[NH_2\cdots CaCO_3H]$	−17.7	−17.2	−18.3
$[NH_2\cdots CaCO_3H\cdots NH_3]$	−22.3	−22.5	−14.2

As the first step of path A, a proton is transferred from nitric acid to $CaCO_3$ through a barrier-less and exothermic reaction to give the complex $[NO_3\cdots CaCO_3H]$ (ΔG = −67.1 kcal/mol, presented in Figure S1). This complex is very stable, and its decomposition requires a significant amount of energy (>150 kcal/mol as computed for the four dissociation reactions presented in Figure S2). It can, however, react with a second molecule of HNO_3 to form a complex, $[NO_3\cdots CaCO_3H_2\cdots NO_3]$ (Figure S3), where a second proton moves from the acid to the basic carbonate. Even in this case, complexation and protonation of carbonate are a concerted and exothermic reaction (by −27.9 kcal/mol), showing no barrier. The complex $[NO_3\cdots CaCO_3H_2\cdots NO_3]$ decomposes into $Ca(NO_3)_2$ and H_2CO_3 (ΔG = −76.9 kcal/mol) with a barrier of 18.1 kcal/mol. $Ca(NO_3)_2$ is one of the reaction products found in experiments.[20−25] Other decomposition reactions are possible, but they are all higher in energy (see Figure S4).

The produced H_2CO_3 is still able to react in two ways (see Table 1 and Figure 1). Indeed, it has been experimentally observed that AN can be destabilized by the presence of acidic species.[29] In the first path, AN in the presence of H_2CO_3 leads to the formation of a complex $[NH_4NO_3\cdots H_2CO_3]$ (ΔG = −63.6 kcal/mol), which evolves into $[NH_3\cdots HNO_3\cdots H_2CO_3]$ (ΔG = −69.6 kcal/mol) through a transition state TS_{3A} with an energetic barrier of 0.8 kcal/mol. In the transition state, a double displacement of protons occurs: one directly from carbonic acid to the nitrate anion and a second one from ammonium to bicarbonate (HCO_3^-), which forms H_2CO_3 again (by an endothermic decomplexation of 3.5 kcal/mol). The other possible reaction for carbonic acid is its decomposition into carbon dioxide and water with a relative free energy of 17.3 kcal/mol. Among these two pathways, the most favorable reaction is the decomposition of H_2CO_3 into H_2O and CO_2, as also indicated by the experimental data.[25−30]

Following path B, calcium carbonate interacts with ammonia, giving the complex $[NH_3\cdots CaCO_3]$ through an exothermic reaction (ΔG = −12.4 kcal/mol) without an energy barrier. This new species, via a transition state TS_{1B} that presents an energetic barrier of 13.1 kcal/mol, leads to a complex $[NH_2\cdots CaCO_3H]$ (Figure S5), releasing an energy equal to −5.9 kcal/mol. Its further decomposition is highly exothermic (>150 kcal/mol), as it can be seen from the data presented in Figure S6. Structural details of the transition states are given in Table S1. This last complex can accept a second molecule of ammonia, giving $[NH_2\cdots CaCO_3H\cdots NH_3]$ (ΔG = −14.2 kcal/mol, Figure S7), which does not undergo further proton displacement. This path B presents less stable complexes than path A, the latter also leading to stable species experimentally observed [as $Ca(NO_3)_2$]. For this reason, path A (i.e., with HNO_3) can be considered as the most favorable.

2.2. Reaction Mechanism between AN and $CaSO_4$.

Because few experimental data are available for the AN/$CaSO_4$ mixture, the reaction mechanism was investigated in analogy to that identified for AN and $CaCO_3$. It is depicted in Scheme 2, and Gibbs free energy profile is reported in Figure 2. The corresponding energy values are detailed in Table 2. As before, the reaction path A corresponds to the reactions between $CaSO_4$ and HNO_3, whereas path B concerns the reaction with NH_3.

As for $CaCO_3$, the first reaction of path A, where HNO_3 simultaneously interacts with the Ca atom and undergoes a proton transfer to SO_4^{2-}, is exothermic and barrier-free, leading to the complex $[NO_3\cdots CaSO_4H]$ (ΔG = −56.8 kcal/mol, Figure S8). The complexation with a second molecule of HNO_3 gives two isomers, namely, $[NO_3\cdots CaSO_4H\cdots HNO_3]_a$ (ΔG = −83.6 kcal/mol) and $[NO_3\cdots CaSO_4H\cdots HNO_3]_b$ (ΔG = −68.1 kcal/mol), depending on the protonation site on the sulfate (see Figure S8). The first isomer evolves into $[NO_3\cdots$

https://dx.doi.org/10.1021/acsomega.9b03964
ACS Omega 2020, 5, 5034−5040

Scheme 2. Pathway of Reactions between AN and $CaSO_4$

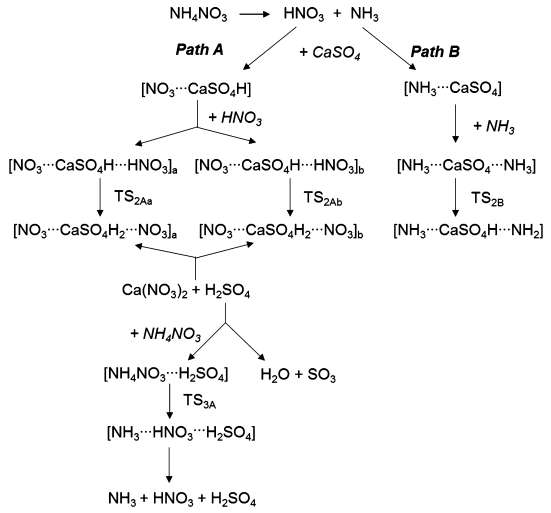

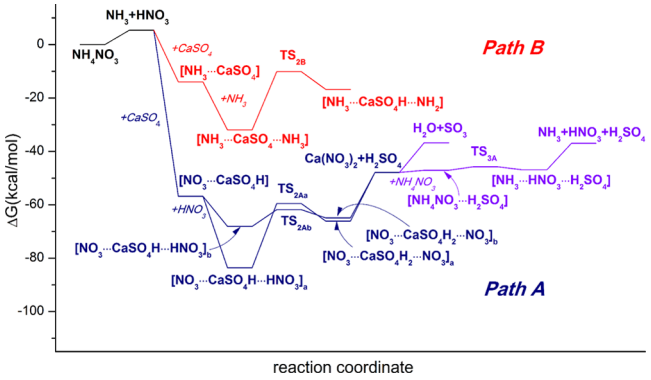

Figure 2. Gibbs free-energy profile for the reaction between AN and $CaSO_4$.

Table 2. Relative Energies (kcal/mol) for the Decomposition Reaction of NH_4NO_3 in the Presence of $CaSO_4$

	ΔE	ΔH	ΔG
NH_4NO_3	0	0	0
$NH_3 + HNO_3$	13.5	14.0	5.4
Path A			
$[NO_3\cdots CaSO_4H]$	−58.6	−57.6	−56.8
$[NO_3\cdots CaSO_4H\cdots HNO_3]_a$	−97.1	−96.1	−83.6
TS_{2Aa}	−74.3	−73.6	−59.5
$[NO_3\cdots CaSO_4H_2\cdots NO_3]_a$	−79.8	−78.8	−66.1
$[NO_3\cdots CaSO_4H\cdots HNO_3]_b$	−82.0	−81.0	−68.1
TS_{2Ab}	−77.2	−76.7	−61.8
$[NO_3\cdots CaSO_4H_2\cdots NO_3]_b$	−78.8	−77.7	−64.9
$Ca(NO_3)_2 + H_2SO_4$	−50.0	−48.9	−47.9
$[NH_4NO_3\cdots H_2SO_4]$	−47.5	−54.0	−47.1
TS_{3A}	−47.3	−53.9	−45.8
$[NH_3\cdots HNO_3\cdots H_2SO_4]$	−47.3	−54.5	−46.9
$NH_3 + HNO_3 + H_2SO_4$	−23.0	−21.0	−37.0
$H_2O + SO_3$	−30.0	−27.6	−36.8
Path B			
$[NH_3\cdots CaSO_4]$	−14.9	−15.2	−14.0
$[NH_3\cdots CaSO_4\cdots NH_3]$	−41.3	−42.0	−32.0
TS_{2B}	−20.5	−21.5	−10.1
$[NH_3\cdots CaSO_4H\cdots NH_2]$	−25.2	−25.0	−16.8

$CaSO_4H_2\cdots NO_3]_a$ (ΔG = −66.1 kcal/mol) passing through the transition state TS_{2Aa} that presents a barrier of 24.1 kcal/mol. The structures of these complexes are reported in Figure 3. Starting from $[NO_3\cdots CaSO_4H\cdots HNO_3]_b$, the other possible

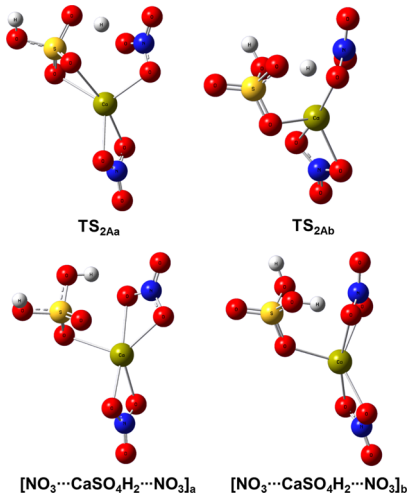

Figure 3. Transition states and complexes of the reactions of HNO_3 and $CaSO_4$.

isomer is $[NO_3\cdots CaSO_4H_2\cdots NO_3]_b$ (ΔG = −64.9 kcal/mol) passing through the transition state TS_{2Ab} with a barrier of 6.3 kcal/mol (see Figure 3). In both cases, the same products, $Ca(NO_3)_2$ and H_2SO_4, are formed. Indeed, the two transition states, TS_{2Aa} and TS_{2Ab}, are both characterized by the displacement of a proton from HNO_3 to $CaSO_4$, albeit from a different site (see Figure 3). More details about these transition states are reported in Table S2.

As previously considered for H_2CO_3, H_2SO_4 is also able to react in two different ways. Indeed, it was experimentally identified as incompatible with AN.[29] In the first path, AN in the presence of H_2SO_4 can lead to the formation of $[NH_4NO_3\cdots H_2SO_4]$ (ΔG = −47.1 kcal/mol), which evolves into the species $[NH_3\cdots HNO_3\cdots H_2SO_4]$ (ΔG = −46.9 kcal/mol) through TS_{3A} with an energetic barrier of 1.3 kcal/mol (see Table 2 for energy values and Figure 2 for Gibbs free energy profile). The transition state presents a double and simultaneous proton displacement from sulfuric acid to nitrate and from ammonium to sulfate. At last, H_2SO_4 is regenerated, producing NH_3 and HNO_3 again with a barrier of 9.9 kcal/mol. The other possibility is the endothermic decomposition of sulfuric acid, which requires 11.1 kcal/mol. So, the catalytic destabilizing effect of H_2SO_4 on AN is in competition with its own decomposition.

Following path B, ammonia reacts with $CaSO_4$ forming a first complex, $[NH_3\cdots CaSO_4]$ (ΔG = −14.0 kcal/mol, Figure S9), with an exothermicity of −19.4 kcal/mol. This first reaction is followed by a similar one, where a second molecule of NH_3 interacts with $[NH_3\cdots CaSO_4]$. The resulting species, $[NH_3\cdots CaSO_4\cdots NH_3]$, is very stable ($\Delta G$ = −32.0 kcal/mol). Although no proton transfer is observed upon the addition of the first ammonia molecule, the interaction with a second NH_3 molecule makes such a reaction possible. The species $[NH_3\cdots CaSO_4H\cdots NH_2]$ (Figure S10) is stable (ΔG = −16.8 kcal/mol), passing through a transition state TS_{2B} with a barrier of 21.9 kcal/mol. Further decomposition of $[NH_3\cdots CaSO_4H\cdots NH_2]$ was not investigated because reaction path B is

https://dx.doi.org/10.1021/acsomega.9b03964
ACS Omega 2020, 5, 5034−5040

energetically less favorable than path A. Furthermore, previous experimental studies on AN's reactivity in the presence of $CaCO_3$[25−30] demonstrated that reactions with HNO_3 were more favored than the ones with NH_3. The same was proved here for $CaSO_4$.

The obtained results clearly indicate that $CaCO_3$ can easily intercept the proton of HNO_3, thus avoiding the decomposition of nitric acid in the highly reactive species. Indeed, the capture of the proton is strongly exothermic (ΔG = −67.1 kcal/mol), whereas the radical production (in pure AN decomposition) is endothermic (ΔG = 40.2 kcal/mol). Moreover, when AN reacts with this stabilizer, there is no production of reactive species ($OH^\bullet$ and $NO_2^\bullet$ radicals) but rather the formation of stable complexes that evolve into stable molecules, such as H_2O, CO_2, and $Ca(NO_3)_2$. These results suggest a direct relationship between the ability of the carbonate to accept the proton from nitric acid and the inhibitor behavior observed experimentally for this additive.

A similar behavior is observed for the reaction with $CaSO_4$, even if the energy release is slightly lower (ΔG = −83.6 kcal/mol for the most stable products) and the proton transfer is less exothermic (ΔG = −56.8 kcal/mol). Other differences between $CaSO_4$ and $CaCO_3$ can be then observed looking at the single reaction steps. For $CaSO_4$, only the first reaction with HNO_3 is spontaneous (ΔG = −56.8 kcal/mol). The second one passes across a proton transfer and two distinct transition states that have a similar relative free energy (ΔG TS_{2Aa} = −59.5 kcal/mol with a barrier of 24.1 kcal/mol and ΔG TS_{2Ab} = −61.8 kcal/mol with a barrier of 6.3 kcal/mol). Therefore, the tendency of $CaSO_4$ to uptake a proton from the second molecule of HNO_3 is lower compared to the one considered for the second protonation of $CaCO_3$. This could explain a less important inhibitor capability than $CaCO_3$.

Finally, the reaction between AN and $CaCO_3$ or $CaSO_4$ leads to similar reaction products: in both cases, $Ca(NO_3)_2$ and a molecule of acid, H_2CO_3 or H_2SO_4. This last step represents another significant difference between $CaCO_3$ and $CaSO_4$ in terms of stabilization effect on AN. Indeed, H_2CO_3 preferentially decomposes into CO_2 and H_2O, whereas H_2SO_4 can decompose into SO_4 and H_2O or react directly with AN.[38] Indeed, this last reaction produces NH_3 and HNO_3 with a barrier of 9.9 kcal/mol, whereas H_2SO_4 decomposes into SO_4 and H_2O with a ΔG of 11.1 kcal/mol. This catalytic effect of H_2SO_4 on AN balances the inhibition effect of $CaSO_4$ issued from the production of stable complexes. This could explain the inert behavior experimentally observed for $CaSO_4$.[20] Indeed, experimental tests have evidenced that the increase of $CaSO_4$ concentration in the AN mixture does not cause an increment of the decomposition temperature.[20]

3. CONCLUSIONS

The detailed computational analysis of the reaction energy profile of AN decomposition in the presence of $CaCO_3$ and $CaSO_4$ not only evidences the molecular mechanisms but also underlines their role as stabilizers in AN formulations. Indeed, both anions, CO_3^{2-} and SO_4^{2-}, capturing an acid proton from AN are able to avoid the production of highly reactive radicals coming from the decomposition of pure AN. These two anions are involved in similar reaction mechanisms, which are characterized by the formation of a stable product, $Ca(NO_3)_2$, and an acid, H_2CO_3 for calcium carbonate and H_2SO_4 for calcium sulfate. However, while carbonic acid decomposes into H_2O and CO_2, sulfuric acid could interact with AN, partially balancing the afore-mentioned stabilizing effect of the deprotonation. These results are in agreement with the experimental observation, $CaSO_4$ presenting a profile more similar to an inert rather than an inhibitor of AN decomposition, the latter clearly observed in the case of $CaCO_3$.

More in general, these results show how modern computational techniques, based on accurate quantum mechanical methods [here density functional theory (DFT)], could help in improving the knowledge on complex reaction mechanisms at the base of compatibility (incompatibility) phenomena.

4. COMPUTATIONAL METHODS

Following previous works on AN decomposition,[22−24] all reaction intermediates were identified using an approach rooted in DFT based on the M06-2X functional[39] and the 6-311+G(2d,2p) basis set.[40] Such a functional provides the most accurate decomposition energies for AN, taking as references the CBS-QB3 values.[22]

The identified intermediates were then characterized as minima (absence of imaginary frequency) or as transition states (one imaginary frequency). Intrinsic reaction coordinate calculations were also performed to confirm that the identified products and reactants were correctly connected by the proposed transition states.[41] Reaction energies, enthalpies, and Gibbs free energies (at 298 K and 1 atm) were computed for all identified reaction intermediates, but only Gibbs free energies will be discussed in the following. More details on the computational approach can be found in the Supporting Information.

All calculations were carried out with the Gaussian program.[42]

■ ASSOCIATED CONTENT

Supporting Information

The Supporting Information is available free of charge at https://pubs.acs.org/doi/10.1021/acsomega.9b03964.

Details of the computational approach, structures of some reaction intermediates and transition states, and decomposition energies of final complexes (PDF)

■ AUTHOR INFORMATION

Corresponding Authors

Patricia Rotureau − *Institut National de l'Environnement Industriel et des Risques (INERIS), 60550 Verneuil-en-Halatte, France*; Email: patricia.rotureau@ineris.fr

Carlo Adamo − *Chimie ParisTech, PSL Research University, CNRS, Institute of Chemistry for Life and Health Sciences (i-CLeHS), FRE 2027, F-75005 Paris, France; Institut Universitaire de France, F-75005 Paris, France;* orcid.org/0000-0002-2638-2735; Email: carlo.adamo@chimie-paristech.fr

Authors

Eleonora Menicacci − *Institut National de l'Environnement Industriel et des Risques (INERIS), 60550 Verneuil-en-Halatte, France; Chimie ParisTech, PSL Research University, CNRS, Institute of Chemistry for Life and Health Sciences (i-CLeHS), FRE 2027, F-75005 Paris, France*

Guillaume Fayet − *Institut National de l'Environnement Industriel et des Risques (INERIS), 60550 Verneuil-en-Halatte, France*

https://dx.doi.org/10.1021/acsomega.9b03964
ACS Omega 2020, 5, 5034−5040

Complete contact information is available at:
https://pubs.acs.org/10.1021/acsomega.9b03964

Notes

The authors declare no competing financial interest.

■ ACKNOWLEDGMENTS

The authors thank Shanti Singh, Richard Turcotte (CERL, Canada), and Guy Marlair (INERIS, France) for the fruitful discussions. The calculations were performed using HPC resources from GENCI-CCRT (Grant 2018-A0030810307).

■ REFERENCES

(1) Rosser, W. A.; Inami, S. H.; Wise, H. The Kinetics of Decomposition of Liquid Ammonium Nitrate. *J. Phys. Chem.* **1963**, *67*, 1753−1757.
(2) Brown, R. N.; McLaren, A. C. On the Mechanism of Thermal Transformation in Solid Ammonium Nitrate. *Proc. R. Soc. London, Ser. A* **1962**, *266*, 329−343.
(3) Keenan, A. G. Differential Thermal Analysis of the Thermal Decomposition of Ammonium Nitrate. *J. Am. Chem. Soc.* **1955**, *77*, 1379−1380.
(4) Gunawan, R.; Zhang, D. Thermal stability and kinetics of decomposition of ammonium nitrate in the presence of pyrite. *J. Hazard. Mater.* **2009**, *165*, 751−758.
(5) Chaturvedi, S.; Dave, P. N. Review on Thermal Decomposition of Ammonium Nitrate. *J. Energ. Mater.* **2013**, *31*, 1−26.
(6) Duh, Y.-S.; Lee, C.; Hsu, C.-C.; Hwang, D.-R.; Kao, C.-S. Chemical Incompatibility of Nitrocompounds. *J. Hazard. Mater.* **1997**, *53*, 183−194.
(7) Karlsen, L. G.; Villadsen, J. Isothermal Reaction Calorimeters-I. A Literature Review. *Chem. Eng. Sci.* **1987**, *42*, 1153−1164.
(8) Brower, K. R.; Oxley, J. C.; Tewari, M. Evidence for Homolytic Decomposition of Ammonium Nitrate at High Temperature. *J. Phys. Chem.* **1989**, *93*, 4029−4033.
(9) Marlair, G.; Kordek, M.-A. Safety and Security Issues Relating to Low Capacity Storage of AN-Based Fertilizers. *J. Hazard. Mater.* **2005**, *123*, 13−28.
(10) Marlair, G.; Michot, C.; Turcotte, R.; Singh, S. Comments about the paper entitled "Lessons to be learned from an analysis of ammonium nitrate disasters in the last 100 years" by Pittman et al. (J. Hazard. Mater. 280 (2014) 472−477. *J. Hazard. Mater.* **2016**, *303*, 177−180.
(11) Babrauskas, V. Explosions of Ammonium Nitrate Fertilizer in Storage or Transportation Are Preventable Accidents. *J. Hazard. Mater.* **2016**, *304*, 134−149.
(12) Menczel, J. D.; Prime, R. B. *Thermal Analysis of Polymers*; John Wiley & Sons, 2014; Vol. *1*, pp 7−240.
(13) Höhne, G.; Hemminger, W.; Flammersheim, H.-J. *Differential Scanning Calorimetry*; Springer Science & Business Media, 2003.
(14) Vold, M. J. Differential Thermal Analysis. *Anal. Chem.* **1949**, *21*, 683−688.
(15) Murphy, C. B. Thermal Analysis. *Anal. Chem.* **1966**, *38*, 443−451.
(16) Zogg, A.; Stoessel, F.; Fischer, U.; Hungerbühler, K. Isothermal Reaction Calorimetry as a Tool for Kinetic Analysis. *Thermochim. Acta* **2004**, *419*, 1−17.
(17) Han, Z.; Sachdeva, S.; Papadaki, M. I.; Mannan, M. S. Ammonium Nitrate Thermal Decomposition with Additives. *J. Loss Prev. Process. Ind.* **2015**, *35*, 307−315.
(18) Han, Z.; Sachdeva, S.; Papadaki, M.; Mannan, M. S. Calorimetry Studies of Ammonium Nitrate - Effect of Inhibitors, Confinement, and Heating Rate. *J. Loss Prev. Process. Ind.* **2015**, *38*, 234−242.
(19) Han, Z.; Sachdeva, S.; Papadaki, M. I.; Mannan, S. Effects of Inhibitor and Promoter Mixtures on Ammonium Nitrate Fertilizer Explosion Hazards. *Thermochim. Acta* **2016**, *624*, 69−75.
(20) Oxley, J. C.; Smith, J. L.; Rogers, E.; Yu, M. Ammonium Nitrate: Thermal Stability and Explosivity Modifiers. *Thermochim. Acta* **2002**, *384*, 23−45.
(21) Oxley, J. C.; Kaushik, S. M.; Gilson, N. S. Thermal Decomposition of Ammonium Nitrate-Based Composites. *Thermochim. Acta* **1989**, *153*, 269−286.
(22) Cagnina, S.; Rotureau, P.; Fayet, G.; Adamo, C. The Ammonium Nitrate and Its Mechanism of Decomposition in the Gas Phase: A Theoretical Study and a DFT Benchmark. *Phys. Chem. Chem. Phys.* **2013**, *15*, 10849−10858.
(23) Cagnina, S.; Rotureau, P.; Fayet, G.; Adamo, C. Modeling Chemical Incompatibility: Ammonium Nitrate and Sodium Salt of Dichloroisocyanuric Acid as a Case Study. *Ind. Eng. Chem. Res.* **2014**, *53*, 13920−13927.
(24) Cagnina, S.; Rotureau, P.; Singh, S.; Turcotte, R.; Fayet, G.; Adamo, C. Theoretical and Experimental Study of the Reaction between Ammonium Nitrate and Sodium Salts. *Ind. Eng. Chem. Res.* **2016**, *55*, 12183−12190.
(25) Rudjak, I.; Kaljuvee, T.; Trikkel, A.; Mikli, V. Thermal behaviour of ammonium nitrate prills coated with limestone and dolomite powder. *J. Therm. Anal. Calorim.* **2009**, *99*, 749−754.
(26) Teir, S.; Eloneva, S.; Fogelholm, C.-J.; Zevenhoven, R. Stability of Calcium Carbonate and Magnesium Carbonate in Rainwater and Nitric Acid Solutions. *Energy Convers. Manag.* **2006**, *47*, 3059−3068.
(27) Popławski, D.; Hoffmann, J.; Hoffmann, K. Effect of Carbonate Minerals on the Thermal Stability of Fertilisers Containing Ammonium Nitrate. *J. Therm. Anal. Calorim.* **2016**, *124*, 1561−1574.
(28) Klimova, I.; Kaljuvee, T.; Türn, L.; Bender, V.; Trikkel, A.; Kuusik, R. Interactions of Ammonium Nitrate with Different Additives. *J. Therm. Anal. Calorim.* **2011**, *105*, 13−26.
(29) Kaljuvee, T.; Edro, E.; Kuusik, R. Influence of Lime-Containing Additives on The thermal Behaviour of Ammonium Nitrate. *J. Therm. Anal. Calorim.* **2008**, *92*, 215−221.
(30) Kaljuvee, T.; Rudjak, I.; Edro, E.; Trikkel, A. Heating Rate Effect on the Thermal Behavior of Ammonium Nitrate and Its Blends with Limestone and Dolomite. *J. Therm. Anal. Calorim.* **2009**, *97*, 215−221.
(31) Zhang, C.; Wang, X.; Huang, H. π-Stacked Interactions in Explosive Crystals: Buffers against External Mechanical Stimuli. *J. Am. Chem. Soc.* **2008**, *130*, 8359.
(32) Sharia, O.; Kuklja, M. M. Modeling Thermal Decomposition Mechanisms in Gaseous and Crystalline Molecular Materials: Application to β-HMX. *J. Phys. Chem. B* **2011**, *115*, 12677.
(33) Zhu, S.-f.; Gan, Q.; Feng, C. Multimolecular Complexes of CL-20 with Nitropyrazole Derivatives: Geometric, Electronic Structure, and Stability. *ACS Omega* **2019**, *4*, 13408−13417.
(34) Zhang, X.-Q.; Yuan, J.-N.; Selvaraj, G.; Ji, G.-F.; Chen, X.-R.; Wei, D.-Q. Towards the low-sensitive and high-energetic co-crystal explosive CL-20/TNT: from intermolecular interactions to structures and properties. *Phys. Chem. Chem. Phys.* **2018**, *20*, 17253−17261.
(35) Molt, R. W.; Watson, T.; Bazanté, A. P.; Bartlett, R. J.; Richards, N. G. J. Gas phase RDX decomposition pathways using coupled cluster theory. *Phys. Chem. Chem. Phys.* **2016**, *18*, 26069−26077.
(36) Xiong, Y.; Ma, Y.; He, X.; Xue, X.; Zhang, C. Reversible intramolecular hydrogen transfer: a completely new mechanism for low impact sensitivity of energetic materials. *Phys. Chem. Chem. Phys.* **2019**, *21*, 2397−2409.
(37) Xia, R.; Wang, J.; Han, Z.; Li, Z.; Mannan, M. S.; Wilhite, B. Mechanism study of ammonium nitrate decomposition with chloride impurity using experimental and molecular simulation approach. *J. Hazard. Mater.* **2019**, *378*, 120585.
(38) Sun, J.; Sun, Z.; Wang, Q.; Ding, H.; Wang, T.; Jiang, C. Catalytic Effects of Inorganic Acids on the Decomposition of Ammonium Nitrate. *J. Hazard. Mater.* **2005**, *127*, 204−210.
(39) Zhao, Y.; Truhlar, D. G. A new local density functional for main- group thermochemistry, transition metal bonding, thermochemical kinetics, and noncovalent interactions. *J. Chem. Phys.* **2006**, *125*, 194101.

https://dx.doi.org/10.1021/acsomega.9b03964
ACS Omega 2020, 5, 5034−5040

(40) Krishnan, R.; Binkley, J. S.; Seeger, R.; Pople, J. A. Self-consistent molecular orbital methods. XX. A basis set for correlated wave functions. *J. Chem. Phys.* **1980**, *72*, 650−654.
(41) Gonzalez, C.; Schlegel, H. B. An improved algorithm for reaction path following. *J. Chem. Phys.* **1989**, *90*, 2154.
(42) Frisch, M. J.; Trucks, G. W.; Schlegel, H. B.; Scuseria, G. E.; Robb, M. A.; Cheeseman, J. R.; Scalmani, G.; Barone, V.; Petersson, G. A.; Nakatsuji, H.; et al. *Gaussian 16*, Revision B.01; Gaussian, Inc.: Wallingford CT, 2016.

https://dx.doi.org/10.1021/acsomega.9b03964
ACS Omega 2020, 5, 5034−5040